# Deformation potentials of the fundamental exciton spectrum of InP

J. Camassel, P. Merle, L. Bayo,* and H. Mathieu

*Centre d'Etudes d'Electronique des Solides,† Université des Sciences et Techniques du Languedoc, 34060-Montpellier Cedex, France*

(Received 27 November 1979)

Wavelength-modulated reflectivity spectra are performed on the direct exciton spectrum of InP under uniaxial-stress conditions. Working at liquid-helium temperature, both the fundamental ($E_0$) and spin-orbit split-off transition ($E_0+\Delta_0$) are investigated. For unstressed crystals, at 5 K the 1$s$ excitons are found at 1418.2 ± 0.5 and 1526.3 ± 0.5 meV, respectively. The spin-orbit splitting energy ($\Delta_0$) is found to be 108 ± 1 meV. Next the stress dependence in configurations $X$ parallel to the [001], [111], and [110] crystallographic axes are investigated. An inability to apply stress magnitudes larger than 3 kbar necessitates analyzing the data with a simple model of orbital-strain interaction which neglects the stress-dependent spin-orbit interaction. Three deformation potentials are deduced: A fully symmetric, interband, deformation potential $C_1+a_1=-8.0\pm0.4$ eV, which gives hydrostatic pressure coefficient $dE_0/dP=11.1\pm0.6$ meV/kbar and two shear deformation potentials, $b=-2.0\pm0.2$ eV and $d=-5.0\pm0.5$ eV. The first one, associated with pure $\Gamma_{12}(2e_{zz}-e_{xx}-e_{yy})$ components of the strain tensor, gives the stress-induced splitting of the valence band under [001] compression while the second, associated with $\Gamma_{15}$ components, corresponds to pure [111] stress. The ratio of experimental splittings in both configurations is related to the anisotropic behavior of the valence band. For InP it is found to be about 0.7.

PACS numbers: 71.25.Tn, 71.70.Ej, 78.20.Hp

## INTRODUCTION

Compared with GaAs, for example, it is well known that very little work has been done on the fundamental properties of the closely related compound InP. In the literature there is a careful study[1] of the excitonic transition $\Gamma_{8v}\rightarrow\Gamma_{6c}$ ($E_0$ transitions) but no effect of uniaxial stress has been reported and the deformation potentials associated with the shift of the band gap and the splitting of the valence band are not known. Up to now, the only published data[2,3] concern the hydrostatic pressure coefficient of the band gap which is found to be about 8.7 or 9.1 meV/kbar according to the results of Ref. 2 or Ref. 3, respectively.

In this work, we give results obtained on large single crystals of InP for uniaxial stress directed along the [100], [111], and [110] crystallographic axes. Two direct transitions $\Gamma_{8v}\rightarrow\Gamma_{6c}$ and $\Gamma_{7v}\rightarrow\Gamma_{6c}$ ($E_0$ and $E_0+\Delta_0$ in the notation of Ref. 4) have been investigated with the help of a high-resolution wavelength-modulated spectrometer. At low temperature, we resolve two excitonic structures and deduce a new and accurate value for the spin-orbit splitting energy. Due to the rather poor crystalline quality of our samples, the uniaxial compressions were restricted to below 3 kbar, and we have not been able to get the weak spin-dependent deformation potentials ($a_2, b_2, d_2$) recently reported for GaP.[4] We analyze our data, taking into account only the orbital-strain interaction, and we deduce three deformation potentials. The first one, $a_1+C_1$, is associated with the hydrostatic components of the strain tensor ($\Gamma_1$ symmetry), the second, $b$, and $d$, are associated with the shear components of respective symmetry $\Gamma_{12}$ ([100] stress) and $\Gamma_{15}$ ([111] stress).

## EXPERIMENTS

The apparatus used in these experiments consisted of a Jobin-Yvon HRS-1 spectrometer, $\lambda$ modulated by a thin vibrating mirror in front of the exit slit. A tungsten lamp and a silicon detector (EGG, SGD 144) completed the setup.

The stress apparatus has been described already and permits application of fairly large uniaxial stresses.[4] In this work, the maximum value reached was only 3 kbar due to the rather poor crystalline quality of InP samples presently available.

All samples used in these experiments were oriented by x-rays and cut from a single ingot of nonintentionally doped crystal.[5] Typical dimensions were about $1\times1\times5$ mm$^3$ with the large dimension along the stress direction. In order to ensure a good stress homogeneity, the two narrow pressure faces were optically flat. Next the large optical faces were carefully polished and chemically etched in $HCl(1)/HNO_3(1)$ for about one min. All spectra were recorded at 5 K.

## RESULTS AND DISCUSSION

### A. Zero-stress experiments

Typical $\lambda$-modulated reflectivity spectra obtained on the $E_0$, $E_0+\Delta_0$ transitions of InP are shown in Fig. 1. Note the small value of the

 

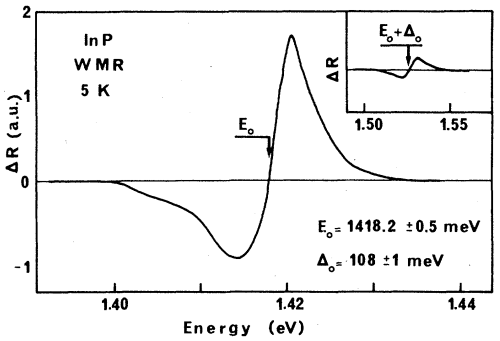


FIG. 1. Wavelength-modulated reflectivity (WMR) spectra obtained at 5 K in the range of $E_0$ and $E_0+\Delta_0$ transitions for InP. The corresponding energies are 1418.2 ($E_0$) and 1426.3 meV ($E_0+\Delta_0$). This gives a spin-orbit splitting energy $\Delta_0 = 108 \pm 1$ meV.

broadening parameter ($\Gamma < 3$ meV) which is associated with the low-temperature. Also note the zero-crossing points. According to the simple theory of first-order derivative spectra,[6,7] they must be associated with the critical energy investigated. In our case, they have been obtained by carefully subtracting a structureless background which always appears in this energy range. The results are fairly reproducible from sample to sample and the corresponding uncertainties range within 0.5 meV. Averaging over a series of 13 different samples, we get at 5 K.

$$E_0 = 1418.2 \pm 0.5 \text{ meV},$$

$$E_0 + \Delta_0 = 1526.3 \pm 0.5 \text{ meV},$$

$$\Delta_0 = 108 \pm 1 \text{ meV}.$$

The first result is in excellent agreement with recent data by Rühle *et al.*[8] (1.41848 eV). Also White *et al.*[9] or Fischbach *et al.*[10] report 1.4182 eV, and, finally, Evangelisti *et al.*[11] report 1.4185 eV. The main discrepancy with the transmission data of Ref. 1 (1.4165 eV at 6 K) comes from the presence of internal strains often present in low-temperature transmission experiments. In this case it is interesting to note that the residual strains present in the samples resulted in a roughly hydrostatic expansion, the associated pressure being of the order of 0.2 kbar.

Concerning the spin-orbit split-off transition ($E_0+\Delta_0$), rather little work has been done. In fact, this is, as far as we know, the first determination obtained at liquid-helium temperature. The value quoted (0.108 eV), is in satisfactory agreement with the result of previous room-temperature determinations.[12,13]

### B. Uniaxial stress experiments

Typical spectra obtained for uniaxial stresses directed in the [100], [111], and [110] directions

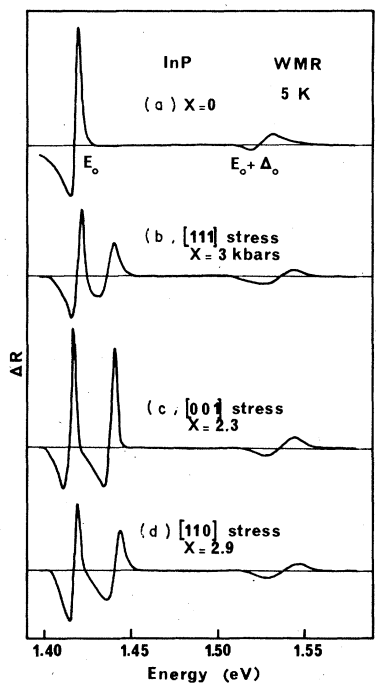


FIG. 2. Stress-induced splitting of the direct exciton spectrum of InP. The lowest transitions $D_1$ ($D_1', D_1''$) appear in both polarizations, $E \| X$ and $E \perp X$, and arise from excitations from the light hole $|\frac{3}{2}, \frac{1}{2}\rangle$ valence band to the lowest conduction band. The next transition $D_2$ ($D_2', D_2''$) appears only in polarization $E \perp X$ and corresponds to direct excitation of an exciton made of a $|\frac{3}{2}, \frac{3}{2}\rangle$ heavy hole and a $\Gamma_1$ electron. The last transitions $D_3$ ($D_3', D_3''$) appear also in both polarizations and correspond to spin-orbit split-off excitons.

are shown in Fig. 2. The stress-induced splitting of the upper valence band ($\Gamma_8$ in double-group notation) is fairly well resolved and permits accurate measurements of the shear deformation potentials (orbital part). This is no longer true for the stress-dependent spin-orbit interaction ($a_2, b_2, d_2$ in the notation of Ref. 4) and we shall neglect it. Working in the notation of Ref. 4, we use the following simplified expressions for the stress dependence of the direct transitions.

#### *1. Stress parallel to [111] direction*

$$D_1 = A_0 - D - 2D^2/(\Delta_0 + D), \tag{1a}$$

$$D_2 = A_0 + D, \tag{1b}$$

$$D_3 = \Delta_0 + A_0 + 2D^2/(\Delta_0 + D), \tag{1c}$$

where $A_0 = (C_1 + a_1)(S_{11} + 2S_{12})X$ and $D = dS_{44}X/2\sqrt{3}$.

In these expressions, $C_1$ and $a_1$ are fully symmetric deformation potentials associated with the hydrostatic stress dependence of the conduction and valence band, respectively. $d$ is a shear deformation potential ($\Gamma_{15}$ symmetry) associated with the stress-induced splitting of the valence band and

$S_{11}, S_{12}, S_{44}$ are elastic compliance constants.

Transition $D_1$ appears first at lower energy and arises from an excitation from the light hole $|\frac{3}{2},\frac{1}{2}\rangle$ valence band to the bottom of the conduction band. The transition is allowed in both polarizations of the incident light with respect to the stress direction ($E \| X$ and $E \perp X$, respectively). This permits an easy identification. The quadratic behavior [see Eq. (1a) and Fig. 3] comes from the stress-induced admixture between the $|\frac{3}{2},\frac{1}{2}\rangle$ and the spin-orbit split-off $|\frac{1}{2},\frac{1}{2}\rangle$ valence bands.

Transition $D_2$ appears at slightly higher energy. It arises from excitations from the $|\frac{3}{2},\frac{3}{2}\rangle$ (heavy hole) valence band to the conduction band. It appears only in polarization ($E \perp X$), and shifts linearly with stress magnitude.

The last transition ($D_3$) arises from the spin-orbit split-off valence band. As $D_1$, it can be found in both polarizations and exhibits a quadratic dependence on stress magnitude.

Experimental data have been collected on a series of six different samples, a typical example being shown in Fig. 3. Also shown is a theoretical curve obtained from Eqs. (1) through a least-mean-square fit procedure. Averaging the series of parameters obtained from the six different measurements, we get the slope parameters listed in Table I ([111] direction).

### 2. *Stress parallel to [001] direction*

We get expressions similar to Eq. (1) but with $B = b(S_{11} - S_{12})X$ replacing $D$.

$$D_1' = A_0 - B - 2B^2/(\Delta_0 + B)\,, \tag{2a}$$

$$D_2' = A_0 + B\,, \tag{2b}$$

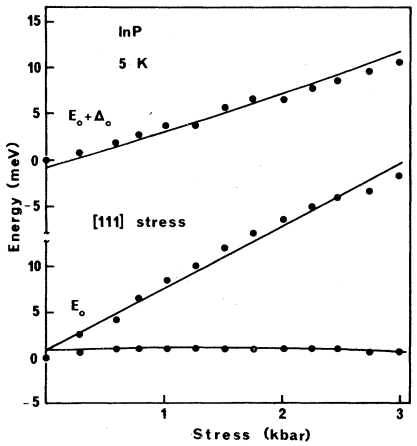


FIG. 3. Stress dependence of the three direct transitions originating from the $\Gamma_{8v} - \Gamma_{7v}$ manifold for $X$ parallel to [111] direction. Full lines: theoretical fit as discussed in the text. Final values obtained for the two parameters $A_0$ and $D$, after averaging over six different samples, are listed in Table I.

$$D_3' = \Delta_0 + A_0 + 2B^2/(\Delta_0 + B)\,. \tag{2c}$$

With respect to the stress direction, the selection rules are not modified and again we find excitation from the $|\frac{3}{2},\frac{3}{2}\rangle$ valence band to the lowest conduction band ($D_2'$) allowed only in polarization $E \perp X$.

A typical stress pattern is shown in Fig. 4. The full lines are again least-square fits through the experimental data, the corresponding parameters (slope parameters) being averaged over different samples as listed in Table I. A comparison of the slope parameters obtained for stress in the [001] direction, with the results obtained for [111] compression, shows the following.

(i) In both cases, we get identical values for the hydrostatic component, $A_0 = 3.7 \pm 0.2$ meV/kbar. It corresponds to a hydrostatic pressure coefficient $dE_0/dP = 11.1 \pm 0.6$ meV/kbar, which must be compared with two slightly different values quoted at room temperature, namely, 8.7 meV/kbar from Ref. 2 and $9.1 + 0.2$ meV/kbar from Ref. 3. However, it is worth noting that the uniaxial stress data is in better agreement with the series already reported for III–V compounds, 11.1 meV/kbar for GaP,[4] and 12.6 meV/kbar for GaAs.[14]

Using the values of $S_{ij}$ parameters extracted from the work of Ref. 15 (in $\text{bar}^{-1}$), $S_{11} = 1.644 \times 10^{-6}$, $S_{12} = -0.594 \times 10^{-6}$, $S_{44} = 2.174 \times 10^{-6}$, we compute a fully symmetric interband deformation potential $C_1 + a_1 = -8.0 \pm 0.4$ eV. It is again in satisfactory agreement with the results reported for GaAs: −8.4 eV (Ref. 16) and GaSb: −8.3 eV (Ref. 17).

(ii) Concerning the splitting of the valence band, we find anisotropic data. Let us consider, for example, the stress pattern displayed in Figs. 3 and 4. In Fig. 3, the lowest transition $D_1$ is almost insensitive to the external pressure up to about 2 kbar. This demonstrates a rather close cancel-

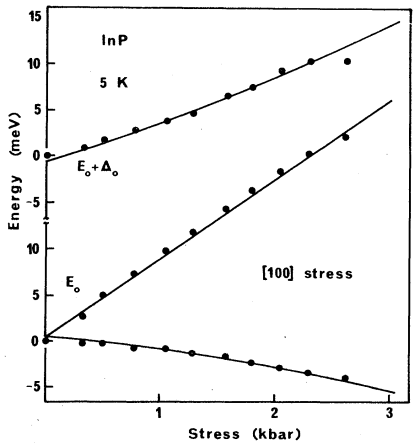


FIG. 4. Same as Fig. 3, but for [100] direction.

TABLE I. Best-fit parameters obtained for InP.

| Stress direction | $E_0$ (meV) | $E_0+\Delta_0$ (meV) | $\Delta_0$ (meV) | $A_0$ (meV/kbar) | $B$ (meV/kbar) | $D$ (meV/kbar) | $F'$ (meV/kbar) |
|---|---|---|---|---|---|---|---|
| [111] | 1418.2 | 1526.5 | 108.3 | $3.7\pm0.2$ | | $3.2\pm0.3$ | |
| [001] | 1418.1 | 1525.9 | 107.8 | $3.7\pm0.2$ | $4.5\pm0.3$ | | |
| [110] | 1418.2 | 1526.4 | 108.2 | $3.6\pm0.6$ | | | $3.5\pm0.5$ |

lation of the positive hydrostatic component $A_0$ by the negation shear component $-D$[see Eq. (1a)]. Indeed we find $A_0=3.7$ and $D=3.2$ meV/kbar. This is no longer true for [001] stress. In Fig. 4, the lowest transition $D_1'$ exhibits a definite negative shift which demonstrates the higher sensitivity of the valence band to the external pressure for this stress direction. The associated coefficient is $B=4.5$ meV/kbar and the corresponding anisotropy ratio $1-\delta E_{[111]}/\delta E_{[001]}\sim 0.3$. It should be noted that this behavior strongly differs from the experimental isotropy recently reported for GaP.[4]

For InP, the deformation potentials associated with [001] and [111] stresses, respectively, are $b=-2.0\pm0.2$ and $d=-5.0\pm0.5$ eV. The corresponding values found for GaP (Ref. 4) are $b=-1.5\pm0.2$ and $d=-4.6\pm0.2$ eV; for GaAs,[16] $b=-1.7\pm0.1$ and $d=-4.55\pm0.25$ eV and, finally, for GaSb,[17] $b=-2.0\pm0.2$ and $d=-4.8\pm0.2$ eV.

### 3. *Stress parallel to [110] direction*

For this stress direction, the nonisotropic splitting of the valence band ($D=0.7B$) should result in nonlinear behavior of the three $D_1''$, $D_2''$, and $D_3''$) components. Indeed, neglecting the hydrostatic components, the shear stress dependence of the $J, M_j$ manifold is obtained from the matrix equation[4]

$$\begin{array}{c} \left|\tfrac{3}{2},\tfrac{3}{2}\right\rangle \quad \left|\tfrac{3}{2},\tfrac{1}{2}\right\rangle \quad \left|\tfrac{1}{2},\tfrac{1}{2}\right\rangle \\ \begin{bmatrix} -F-E & -\sqrt{3}(B-D)/4 & \sqrt{6}(B-D)/4 \\ -\sqrt{3}(B-D)/4 & F-E & \sqrt{2}F \\ \sqrt{6}(B-D)/4 & \sqrt{2}F & -\Delta_0-E \end{bmatrix} \end{array} = 0 , \tag{3}$$

where $F=(B+3D)/4$.

Diagonalizing first the $2\times2$ matrix associated with the $\Gamma_8$ valence band and working next in first-order perturbation theory, we find

$$V_1=F'+\beta^2/\Delta_0, \tag{4a}$$

$$V_2=-F'+\beta'^2/\Delta_0, \tag{4b}$$

$$V_3=-\Delta_0-\beta^2/\Delta_0-\beta'^2/\Delta_0, \tag{4c}$$

where

$$F'=(B^2+3D^2/2)^{1/2},$$

$$\beta=\sqrt{6}(B-D)(2F-F')/[3(B-D)^2+16(F-F')^2]^{1/2},$$

$$\beta'=\sqrt{2}[3(B-D)^2 -16F(F-F')]/4[3(B-D)^2+16(F-F')^2]^{1/2}.$$

These expressions show the following.

(i) The $\Gamma_8$ manifold ($V_1$ and $V_2$ bands) should open with a linear rate $(B^2+3D^2)^{1/2}$. Using the experimental results obtained in the [111] and [100] directions, we compute a theoretical slope $F'=3.6$ meV/kbar which must be compared with the value $F=(B+3D)/4$ expected in the limit of very weak anisotropy.[4] We find $F=3.5$ meV/kbar.

The comparison of both predictions shows that strong experimental evidence of the valence-band anisotropy is not to be expected from the splitting of the valence band in the [110] direction. This is true even with anisotropy ratios $\alpha=1-D/B$ as large as 0.3. The reason is simple. Expanding the energy difference $F-F'$ versus $\alpha$, we do not find a first-order term, but only a weak second-order contribution ($-3\alpha^2/8$) which can be neglected for most practical purposes.

(ii) Concerning the nonlinear behavior of the $\Gamma_8$ manifold, we find that both valence bands ($V_1, V_2$) should behave nonlinearly but with different rates. Since the first one ($V_1$) was already strongly coupled with the spin-orbit valence band, it will not be drastically modified. In this case, the only noticeable effect should come from $V_2$. We have computed the corresponding contribution for InP and find a departure from linearity of only 0.2 meV at about 3 kbar. This is far below our range of uncertainty. In this case we can safely use the approximate expressions

$$D_1''=A_0-F'-2F^2/\Delta_0, \tag{5a}$$

$$D_2''=A_0+F'-6(B-D)^2/16\Delta_0, \tag{5b}$$

$$D_3''=\Delta_0+2F^2/\Delta_0+6(B-D)^2/16\Delta_0. \tag{5c}$$

Experimental data are shown in Fig. 5. Averaging over a series of five different samples, we find $A_0=3.6$ meV/kbar and $F'=3.5\pm0.5$ meV/kbar, both of which are in excellent agreement with the results found in [111] and [001] directions.

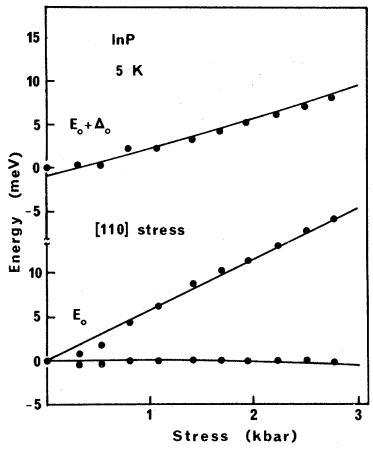


FIG. 5. Same as Fig. 3, for [110] direction.

## CONCLUSIONS

We have investigated the direct exciton spectrum of InP. At liquid-helium temperature, we measure accurate energy positions for the $E_0$, $E_0+\Delta_0$ transitions and deduce a spin-orbit splitting energy $\Delta_0 = 108 \pm 1$ meV. We concentrate next on the uniaxial stress dependence of both excitonic transitions. We deduce three deformation potentials. An interband deformation potential $C_1 + a_1 = -8.0 \pm 0.4$ eV, which is totally symmetric and corresponds to a hydrostatic pressure coefficient $dE_0/dP = 11.1 \pm 0.6$ meV/kbar and two shear-strain deformation potentials, $b = -2.0 \pm 0.2$ eV and $d = -5.0 \pm 0.5$ eV, which are associated with pure [001] and [111] strains, respectively.

*Note added in proof.* Since the completion of this work, we have been aware of an independent determination reported by G. Weber and W. Ruhle [Phys. Status Solidi 92B, 425 (1979)]. In their experiments, restricted to the fundamental $E_0$ reflectivity spectrum and 1.5 kbar, they found 6.6, −1.55, and −4.2 eV for $a$, $b$, and $d$ deformation potentials, respectively. All values are quoted with 15% error bars.

*Permanent address: Dept. Electricitat i Electronica, Universitat Autonoma de Barcelona, Spain.
†Laboratoire associé au CNRS.

[1]W. J. Turner, W. E. Reese, and G. D. Pettit, Phys. Rev. 136, A1467 (1964).
[2]R. Zallen and W. Paul, Phys. Rev. 155, 703 (1967).
[3]R. A. Bendoryus and A. Y. Shileika, Fiz. Tekh. Poluprovodn. 6, 1185 (1972) [Sov. Phys. Semicond. 6, 1042 (1972)].
[4]H. Mathieu, P. Merle, E. L. Ameziane, B. Archilla, J. Camassel, and G. Poiblaud, Phys. Rev. B 19, 2209 (1979).
[5]Cambridge Instruments Company, Centre d'Affaires Paris-Nord, 93153 Le Blanc Mesnil.
[6]J. Camassel, D. Auvergne, and H. Mathieu, J. Appl. Phys. 46, 2683 (1975).
[7]B. Batz, Semicond. Semimet. 9, 316 (1972).
[8]W. Ruhle and W. Klingenstein, Phys. Rev. B 18, 7011 (1978).
[9]A. M. White, P. J. Dean, L. L. Taylor, R. C. Clarke, D. J. Ashen, and J. B. Mullin, J. Phys. C 5, 1727 (1972).
[10]J. U. Fishbach, G. Benz, M. Stath, M. M. Pilkuhn, and K. W. Benz, Solid State Commun. 11, 721 (1972).
[11]F. Evangelisti, F. W. Fischbach, and A. Frova, Phys. Rev. B 9, 1516 (1974).
[12]M. Cardona, K. L. Shaklee, and F. H. Pollak, Phys. Rev. 154, 696 (1967).
[13]C. Alibert, G. Bordure, A. Laugier, and J. Chevallier, Phys. Rev. B 6, 1301 (1972).
[14]B. Welber, M. Cardona, C. K. Kim, and S. Rodriguez, Phys. Rev. B 12, 5729 (1975).
[15]F. S. Hickernell and W. R. Gayton, J. Appl. Phys. 37, 462 (1966).
[16]M. Chandrasekhar and F. H. Pollak, Phys. Rev. B 15, 2127 (1977).
[17]R. A. Noack, W. Ruhle, and T. N. Morgan, Phys. Rev. B 18, 6944 (1978).